Asian Journal of Chemistry; Vol. 33, No. 9 (2021), 2191-2202

ASIAN JOURNAL OF CHEMISTRY

https://doi.org/10.14233/ajchem.2021.23339

Exploration of Theoretical and Antioxidant Mimetic Activities of Binuclear Copper(II) and Nickel(II) Coordination Complexes

BHARTI MOHAN and MUKESH CHOUDHARY*

Department of Chemistry, National Institute of Technology Patna, Patna-800005, India

*Corresponding author: E-mail: mukesh@nitp.ac.in

Received: 28 May 2021; *Accepted*: 16 July 2021; *Published online*: 20 August 2021; AJC-20483

Three dinuclear copper(II) and nickel(II) complexes *viz*. $[Cu_2(L_a)(py)_2]\cdot(ClO_4)_2$ (**1**), $[Ni_2(L_b)(ImH)_2]\cdot(ClO_4)_2$ (**2**) and $[Ni_2(L_c)(H_2O)_2]\cdot(ClO_4)_2$ (**3**) were designed and synthesized using disulfide and auxiliary ligands as functional models for antioxidant superoxide dismutase enzyme (where, H_2L_a-H_2L_c = disulfide ligands bearing S-S bond, py = pyridine, ImH = imidazole). The disulfide ligands were synthesized by condensation reaction of 2-(2-(2-aminophenyl)disulfanyl)benzeneamine with 3-bromo-2-hydroxy-5-nitrobenzaldehyde; 5-bromo-2-hydroxybenzaldehyde and 3,5-dichloro-2-hydroxybenzaldehyde, respectively. All the compounds were characterized by various spectrometry methods. The molecular docking study was performed against penicillin binding protein 4 (PBP4) active site pocket and *E. coli* DNA Gyrase B ATPase domain to evaluate the possible mechanism of antibacterial property of disulfide ligands. The results revealed that H_2L_a-H_2L_c possess higher binding affinity for active site of PBP4 and Gyrase B ATPase domain. The present study also demonstrated that disulfide compounds have potential to inhibit the PBP4 and Gyrase B ATPase domain and can be developed as lead compounds. In addition, antioxidant superoxide dismutase (SOD) activity is also discussed of these complexes. The antioxidant superoxide measurements show that complexes behave as superoxide mimic in alkaline nitro blue tetrazolium chloride (NBT) assay.

Keywords: Dinuclear metal(II) complexes, Antioxidant activities, Disulfide, Auxiliary ligands, Pyridine, Imidazole.

INTRODUCTION

Metal-disulfide interactions play an important role in the high functionality of Cu,Zn-superoxide dismutase ((SOD) enzyme and metalloenzymes have been a subject of considerable interest for many years [1,2]. This is because of the versatility of metal-disulfide interactions arising from the redox active nature of both metal and disulfide, which results in the formation of a variety of coordination species such as M(II) with bridging thiolates or disulfides [3-5]. Disulfide bond formation is essential for the activity of Cu,Zn-SOD and is accelerated greatly in the presence of O2 and Cu-sulfur-rich proteins [6-10].

Superoxide dismutase (SOD) is one of the most important antioxidant enzymes that neutralize superoxide by converting it to H_2O_2 and O_2. Several low molecular weight mimics, especially, Cu(II) and Ni(II) complexes, have been shown to exhibit the ability to efficiently catalyze superoxide dismutation. So it has been expected that metal complexes as antioxidants can be a better alternative to act as SOD mimics [11-16]. To get insight into metal-disulfide interactions, which are more relevant to the biological systems, reaction of copper(II) and nickel(II) ions with disulfide and auxiliary ligands are highly desirable to be investigated. Herein, we report the synthesis and characterization of copper(II) and nickel(II) complexes with disulfide and auxiliary ligands, which can be considered as antioxidant mimetic models for Cu,Zn-SOD enzymes. Furthermore, little attention has been focused on the influence of auxiliary ligands involved in metal-disulfide system. Remarkably, the use of pyridine/imidazole/water molecule as auxiliary ligands in this metal-disulfide system led to the formation of dimetal(II) complexes with a disulfide-type ligands (Fig. 1) that links two metal centers.

EXPERIMENTAL

The chemicals used were of AnalaR grade. The chemicals *viz*. 3-bromo-2-hydroxy-5-nitrobenzaldehyde, 5-bromo-2-hydroxybenzaldehyde, 3,5-dichloro-2-hydroxybenzaldehyde, copper(II) perchlorate hexahydrate, nickel(II) perchlorate

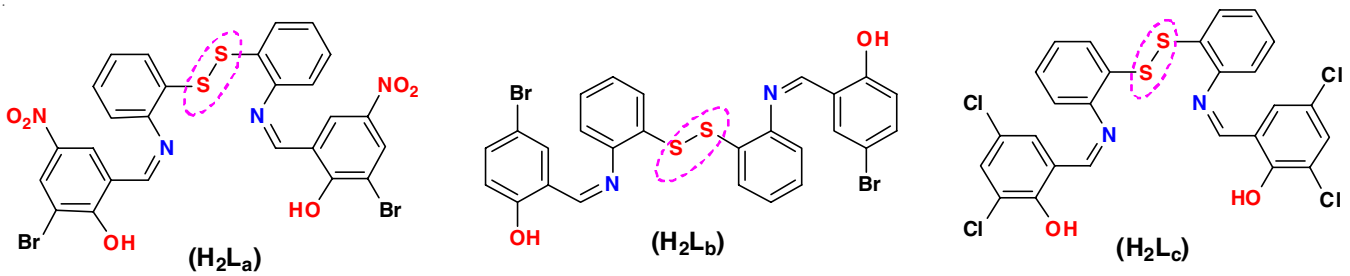

Fig. 1. Representative structures of the disulfide derivatives

hexahydrate were purchased from Sigma-Aldrich Company. All reagents and solvents were dried before use according to standard methods.

Characterization: The instrumental techniques employed for the characterization of the newly synthesized compounds include FTIR and UV-Vis spectroscopy, ^{1}H & ^{13}C NMR. The UV-Vis spectra were recorded at 25 ºC on a Thermo scientific UV-Vis recording spectrophotometer Evolution-3000 in quartz cells. IR spectra were recorded in KBr medium on a Shimadzu IR Affinity-1S Fourier transform infrared spectrophotometer. NMR spectra were recorded on a Bruker Ultrashield 500 plus 400 MHz FT-NMR Spectrometer. FAB mass spectra were recorded on a JEOL SX 102/DA 6000 mass spectrometer using xenon (6kV, 10mA) as the FAB gas. The accelerating voltage was 10 kV and the spectra were recorded at room temperature (RT) with m-nitro benzoyl alcohol as the matrix.

Preliminary test: To be effective as a drug candidates, the preliminary test in the potential application for theoretical biological activities of disulfide ligands and their corresponding complexes (**1-3**) had been evaluated by SwissADME: a web tool to evaluate pharmacokinetics, drug likeness and medicinal chemistry friendliness of small molecules [17].

Superoxide dismutase activity determination: The antioxidant SOD-like activities of studied disulfide ligands and their corresponding metal(II) complexes were investigated by NBT-DMSO assay. The *in vitro* SOD activity was measured using alkaline DMSO as a source of superoxide radical (O_2^-) and nitrobluetetrazolium chloride (NBT) as O_2^- scavenger [11]. A sample (400 µL) to be assayed was added to a solution containing 2.1 mL of 0.2 M potassium phosphate buffer (pH 8.6) and 1 mL of 56 µM of alkaline DMSO solution was added while stirring. The absorbance was then monitered at 540 nm against a sample prepared under similar condition except NaOH was absent in DMSO. A unit of superoxide dismutase (SOD) activity is the concentration of complex, which causes 50% inhibition of alkaline DMSO mediated reduction of nitrobluetetrazolium chloride (NBT).

Antibacterial activity: The *in vitro* antibacterial activities of disulfide ligands and their corresponding metal(II) complexes were screened against two bacteria (*E. coli* and *S. typhi*) by agar-well diffusion method [12,13] using nutrient agar as the medium and chloramphenicol as control. The antibiotics chloramphenicol was used as a positive control against bacterial species. Dimethyl sulfoxide (DMSO) was used as solvent control. Each of the complexes was dissolved in DMSO and the solutions of three concentrations (10-20 mM) were prepared separately. *E. coli* and *S. typhi* test cultures were first spread into the surface of sterilized Mueller-Hinton agar plates using sterile cotton swabs. Three wells were made on each plate with a sterile cork borer instrument. The potent among the serially diluted test compounds were chosen for agar-well diffusion. Each compounds (15 µg) in DMSO (< 5%) were added in one well of each plate. All of the plates were then covered with lids and incubated at 37 ºC for 24 h. After incubation, plates were observed for the zone of bacterial growth inhibition. The size of inhibition zones was measured and antibacterial activity of the disulfide ligands and their corresponding complexes were expressed in terms of an average diameter of inhibition zone in millimeters.

Synthesis of Schiff base ligands: The ligands were synthesized according to the following procedures:

Synthesis of H_2L_a: Compound H_2L_a was synthesized by refluxing 2-(2-(2-aminophenyl)disulfanyl)benzeneamine (**L**) (2.485 g, 10.0 mmol) with 3-bromo-2-hydroxy-5-nitrobenzaldehyde (4.920 g, 20 mmol) in a molar ratio 1:2 in CH_2Cl_2 as solvent in the presence of *p*-toluene sulphonic acid (*p*-TSA) as a dehydrating agent. The progress of reaction was closely examined with the help of TLC. On cooling the solution to room temperature, cream solid was obtained, which were filtered off, washed with methanol and ether, and dried *in vacuo* over fused $CaCl_2$. Yield: 0.632 g (85%). m.p.: 310-320 ºC. Anal. calcd. (found) % for $C_{26}H_{16}N_4O_6S_2Br_2$: C, 44.33 (44.34); H, 2.29 (2.30); N, 7.95 (7.96). FAB-mass (*m/z*): Found (calcd.): 706.38 (705.00). ^{1}H NMR (400 MHz, DMSO-d_6) δ ppm: 12.53 (s, 2H, -OH), 8.59 (s, 2H, -N=CH), 7.97-7.96 (m, 4H, Ar-H), 7.69-7.68 (m, 2H, Ar-H), 7.65-7.63 (m, 2H, Ar-H), 7.59-7.55 (m, 4H, Ar-H). ^{13}C NMR (DMSO-d_6, 100 MHz) δ ppm: 163.53, 152.76, 147.47, 132.80, 132.69, 130.74, 129.10, 128.89, 128.25, 123.40, 121.96, 121.26.

Synthesis of H_2L_b: A solution of 5-bromo-2-hydroxybenzaldehyde (4.021 g, 20.0 mmol) in 20 mL of absolute ethanol at 60 ºC was slowly added to a solution of 2-(2-(2-aminophenyl)disulfanyl)benzeneamine (2.485 g, 10.0 mmol) in 20 mL of absolute ethanol/CH_2Cl_2 at 60 ºC and the mixture stirred for 10 h at 60 ºC. The purity of compound was examined with the help of TLC. The mixture was then cooled, and absolute ethanol (60 mL) was added. The mixture was stirred for 15 min and then filtered off. The filtrate volume reduced to about 10 mL and resulting in the formation of a brown precipitate. The precipitate was decanted off, washed twice with ethanol (2 × 10 mL) and dried *in vacuo* at room temperature and stored in a $CaCl_2$ desiccator. Yield: 0.453 g (80%); m.p.: 295-298 ºC. Anal. calcd. (found) % for $C_{26}H_{18}N_2O_2S_2Br_2$: C, 50.83 (50.84);

H, 2.95 (2.96); N, 4.56 (4.57). FAB-mass (*m/z*): Found (calcd.): 614.37 (614.00). ^{1}H NMR (400 MHz, DMSO-d_6) δ ppm: 12.52 (s, 2H. -OH), 8.58 (s, 2H, -N=CH), 7.96 (d, *J* = 8.0 Hz, 2H), 7.67 (d, *J* = 8.0 Hz, 1H), 7.64-7.62 (t, *J* = 4.0 Hz, 2H), 7.56 (t, *J* = 8.0 Hz, 2H). ^{13}C-NMR (100 MHz, DMSO) δ ppm: 163.56, 152.80, 147.51, 132.84, 132.73, 130.77, 129.14, 128.93, 128.28, 123.44, 122.00, 121.30, 40.68, 40.47, 40.26, 40.05, 39.84, 39.63, 39.42.

Synthesis of H_2L_c: 3,5-Dichloro-2-hydroxybenzaldehyde (3.820 g, 20 mmol) in 20 mL of absolute ethanol was slowly added to a solution of 2-(2-(2-aminophenyl)disulfanyl)benzeneamine (2.485 g, 10.0 mmol) in 20 mL of absolute ethanol and heated the reaction mixture on a water bath at 58 ºC for 7 h. The progress of reactions were closely examined with the help of TLC. On cooling the solution to room temperature, dark brown color product was obtained, which were filtered off, washed with methanol and dried *in vacuo* over fused $CaCl_2$. Yield: 0.378 g (75%). m.p.:290-310 ºC. Anal. calcd. (found) % for $C_{26}H_{16}N_2O_2S_2Cl_4$: C, 52.54 (52.55); H, 2.71 (2.72); N, 4.71 (4.70). FAB-mass (*m/z*): Found (calcd) %: 594.36 (594.00).

Synthesis of binuclear metal(II) complexes: Binuclear metal(II) complexes were synthesized according to the following general procedure:

Synthesis of $[Cu_2(L_a)(py)_2]\cdot(ClO_4)_2$ complex (1): Triethylamine (3.0 mmol, 40 µL) as base dissolved in 25 mL methanol, H_2La (1.0 mmol, 0.706 g) and $Cu(ClO_4)_2\cdot6H_2O$ (1.0 mmol, 0.345 g) dissolved in 50 mL CH_3OH were mixed together. To this reaction mixture, pyridine (py) (2.0 mmol, 0.158 µL) was added. After 4 h reflux, the brown precipitate was separated and washed with hot methanol. Yield: 0.428 g (68%). Anal. calcd. (found) % for $C_{36}H_{24}N_6O_{14}S_2Br_2Cl_2Cu_2$: C, 36.74 (36.75); H, 2.06 (2.07); N, 7.14 (7.15). FAB-mass (*m/z*): Found (calcd): 1171.00 (1176.84).

Synthesis of $[Ni_2(L_b)(ImH)_2]\cdot(ClO_4)_2$ complex (2): This complex was obtained by similar method as reported for complex **1** by employing H_2L_b (1.0 mmol, 0.614 g) and imidazole (2.0 mmol, 1.361g) instead of H_2L_a and pyridine. Yield: 0.573 (70%). Anal. calcd. (found) % for $C_{32}H_{24}N_6O_6S_2Br_2Cl_2Ni_2$: C, 38.40 (38.41); H, 2.42 (2.43); N, 8.40 (8.41). FAB-mass (*m/z*): Found (calcd): 995.00 (1000.80).

Synthesis of $[Ni_2(L_c)(H_2O)_2]\cdot(ClO_4)_2$ complex (3): To a methanolic solution of ligand H_2L_c (1 mmol, 0.594 g), $Ni(ClO_4)_2\cdot6H_2O$ (1.0 mmol, 0.365 g) were added in the presence of triethylamine (3.0 mmol, 40 µL) as base. The mixture was stirred at room temperature for 3 h. A light green precipitate was separated and washed with hot methanol. Yield: 0.528 g (65%). Anal. calcd. (found) % for $C_{26}H_{18}N_2O_{12}S_2Cl_6Ni_2$: C, 33.06 (33.07); H, 1.92 (1.93); N, 2.97 (2.98). FAB-mass (*m/z*): Found (calcd): 939.71 (944.66).

RESULTS AND DISCUSSION

Characterization of the disulfide ligands and their corresponding metal(II) complexes were carried out using spectroscopic methods. In the first step, H_2L_a-H_2L_c were synthesized by the reaction between 2-(2-(2-aminophenyl)disulfanyl)benzeneamine with 3-bromo-2-hydroxy-5-nitrobenzaldehyde/5-bromo-2-hydroxybenzaldehyde/3,5-dichloro-2-hydroxybenzaldehyde with the ratio of 1:2 to form the corresponding disulfide ligands. Finally, disulfide ligands (**H_2L_a-H_2L_c**) were reacted with $Cu(ClO_4)_2\cdot6H_2O$/$Ni(ClO_4)_2\cdot6H_2O$ and two molecules of auxiliary ligands (pyridine/imidazole/water) to afford dimer binuclear metal(II) complexes (**Scheme-I**).The obtained complexes were microcrystalline solids and stable in air with melting points above 200 ºC. The elemental analyses were in agreement with the chemical formula proposed for proposed structures.

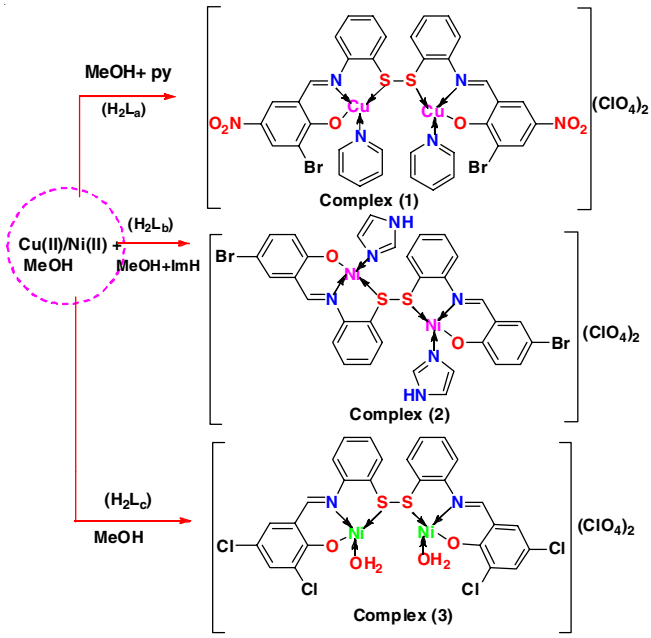

Scheme-I: Synthetic route of the novel disulfide Schiff base metal(II) complexes (**1-3**)

NMR studies: The ^{1}H NMR spectrum of free disulfide derivatives (**H_2L_a-H_2L_c**) were recorded in DMSO-d_6 using TMS as internal standard. A representative ^{1}H NMR spectrum data to support characterization of disulfide compound have been shown in Fig. 2. The ^{13}C{^{1}H}-NMR spectral data is provided in Fig. 3. In ^{1}H NMR, all peaks for compounds **H_2L_a-H_2L_c** have been successfully assigned. NMR data has been recorded in DMSO-d_6 solvent against tetramethylsilane (TMS) as internal reference for all the compounds. The ^{1}H NMR spectra of the prepared compounds (**H_2L_a-H_2L_c**) had shown signals for aromatic protons and hydroxyl and azomethine protons. The ^{1}H NMR spectra of the representative compounds displayed the Ar-OH protons and aromatic protons at 12.53-14.51 and 7.97-7.96 ppm, respectively. Azomethine protons (-N=CH) in studied compounds (**H_2L_a-H_2L_c**) appeared at 8.59-8.72 ppm.

FTIR studies: The key FTIR bands of disulfide ligands (H_2L_a-H_2L_c) were compared with its binuclear metal(II) complexes (Table-1). The IR spectra of disulfide ligands (**H_2L_a-H_2L_c**) exhibit strong bands at the range 1618-1610 cm^{-1}, which is the characteristics of diazomethine (>C=N) group. Furthermore, the IR spectra data confirmed the coordination of disulfide ligands (**H_2L_a-H_2L_c**) through diazomethine nitrogen to the metal atoms by shifting the ν(C=N) stretching frequency of free disulfide derivatives to the higher frequency in the range of 1642-1628 cm^{-1} in binuclear metal(II) complexes (**1-3**). Further-

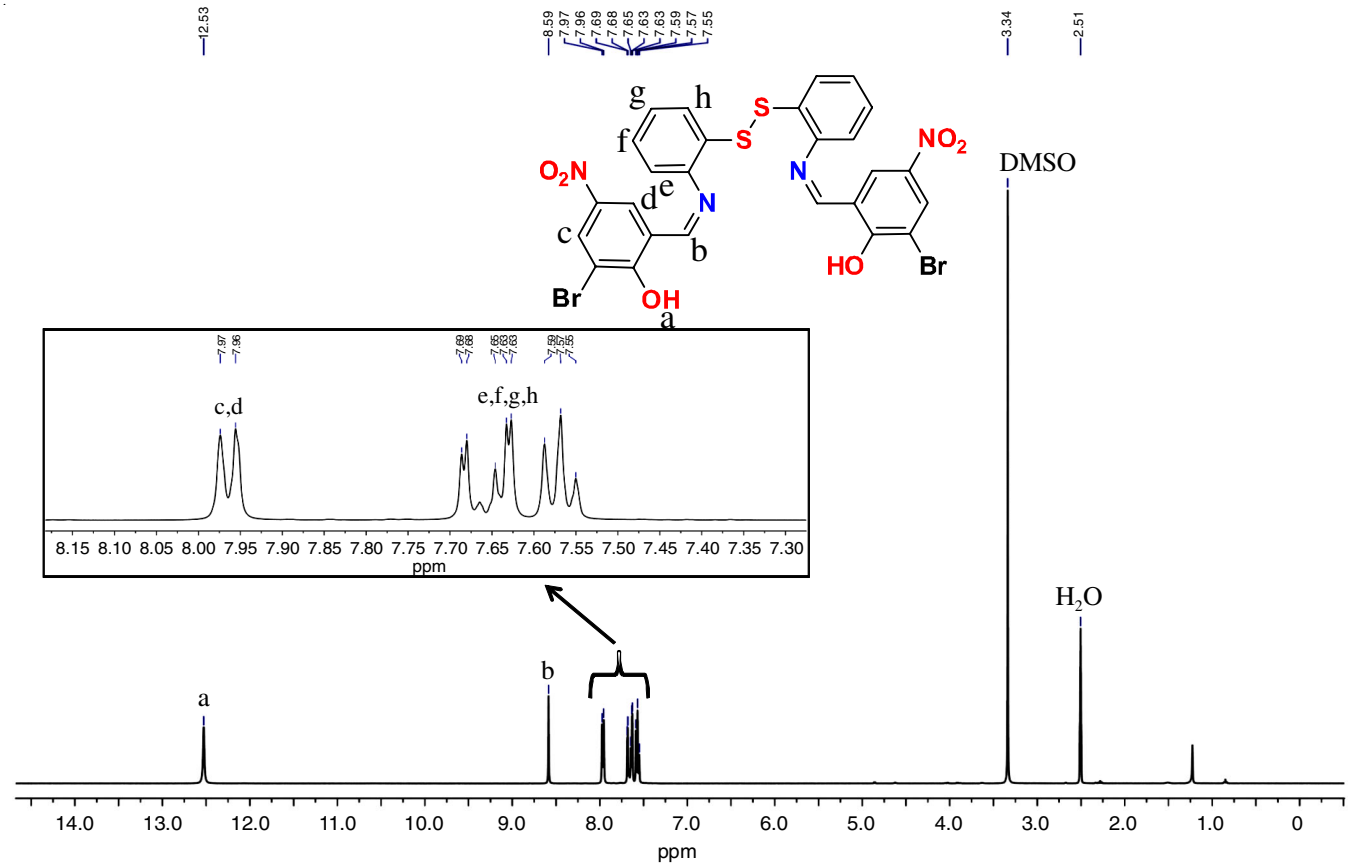

Fig. 2. ^{1}H NMR spectrum of $\mathbf{H_2L_a}$

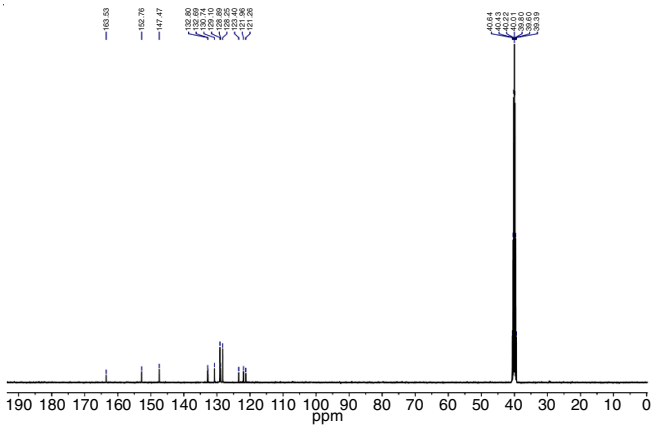

Fig. 3. ^{13}C NMR spectrum of $\mathbf{H_2L_a}$

more, the spectra of disulfide ligands ($\mathbf{H_2L_a}$-$\mathbf{H_2L_c}$) showed a broad band at the range 3448-3436 cm^{-1}, attributed to the stretching vibrations of the phenolic ν(Ar–OH) group, which were absent in the spectra of binuclear metal(II) complexes (**1**-**3**). The new bands at 732 and 735 cm^{-1} for $\mathbf{H_2L_a}$, 728 and 733 cm^{-1} for $\mathbf{H_2L_b}$, 726 and 730 cm^{-1} for $\mathbf{H_2L_c}$, were assigned to C-S *str*. Moreover, new bands assigned to ν(S-S) [18] at 523 and 529 cm^{-1}($\mathbf{H_2L_a}$), 536 and 539 cm^{-1}($\mathbf{H_2L_b}$), 547 and 552 cm^{-1}($\mathbf{H_2L_c}$) are found , in agreement with disulfide S-S bond. Band in the region of 492-472 cm^{-1}, 547-521 cm^{-1} and 786-739 cm^{-1} in the binuclear metal(II) complexes, which may be assigned to the ν(M–O), ν(M–N) and ν(M–S), respectively. While in the IR spectra of binuclear metal(II) complexes (**1**-**3**), the broad band around 1365 and 643 cm^{-1}, 3377 and 1486 cm^{-1}, 3450 and 840 cm^{-1}, can be attributed to pyridine, imidazole and water molecules in the binuclear metal(II) complexes (**1**-**3**), respectively. The IR spectra showed that the disulfide ligands were coordinated to the metal ions in a hexadentate-$O_2N_2S_2$ manner.

UV-Vis studies: The UV-Vis spectra of complexes were recorded in methanol and are presented in Fig. 4. The electronic

TABLE-1
INFRARED CHARACTERISTICS BAND FREQUENCIES (cm^{-1}) OF THE $\mathbf{H_2L_a}$-$\mathbf{H_2L_c}$ AND ITS METAL COMPLEXES

Ligand/ complex	Frequency (cm^{-1})									
	C=N	C=C	C-H	Ar-H	C-S	S-S	O-H	M-O	M-N	M-S
$\mathbf{H_2L_a}$	1610	1420-1560	2916	3052	732, 735	523, 529	3436	–	–	–
$\mathbf{H_2L_b}$	1613	1428-1530	2919	3056	728, 733	536, 539	3442	–	–	–
$\mathbf{H_2L_c}$	1618	1452-1580	2922	3059	726, 730	547, 552	3448	–	–	–
Complex **(1)**	1628	1471-1482	2942	3066	–	585, 587	–	472	521	739
Complex **(2)**	1634	1478-1494	2893	3073	–	572, 576	–	487	533	783
Complex **(3)**	1642	1480-1496	2968	3086	–	584, 592	–	492	547	786

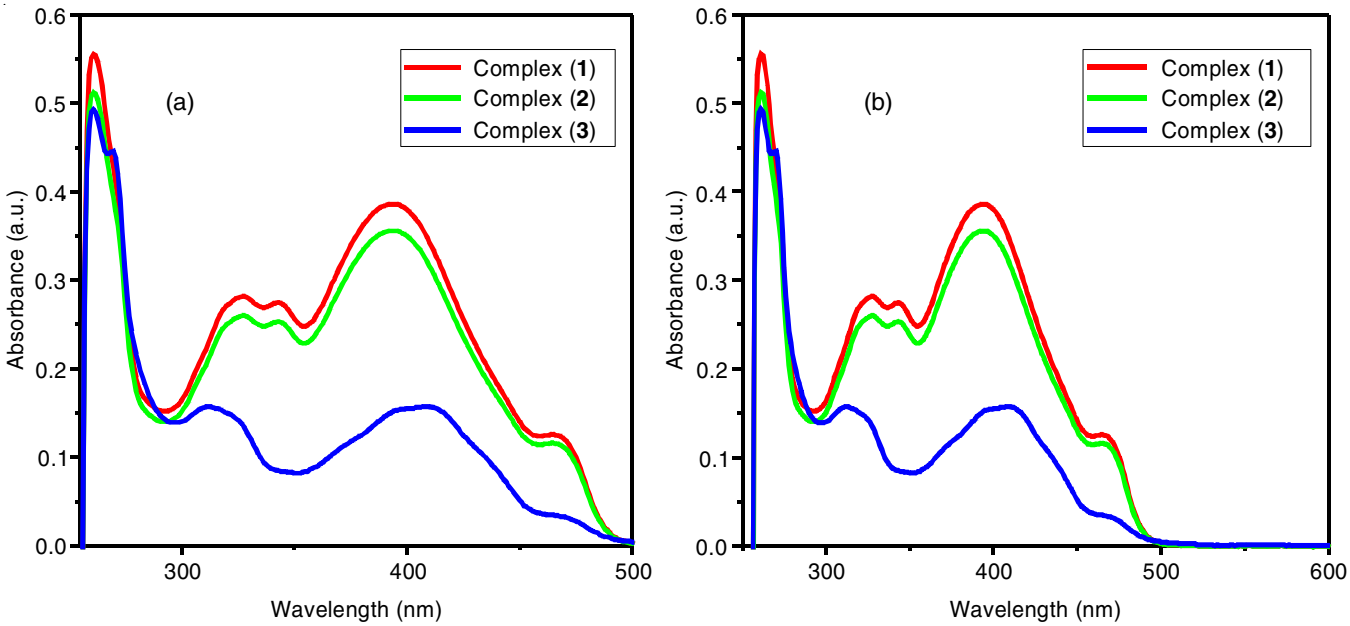

Fig. 4. Absorption spectra (1×10^{-6} M) of metal(II) complexes (**1**-**3**) in the range: 250-500 nm and 250-600 nm

spectra of disulfide ligands ($\mathbf{H_2L_a}$-$\mathbf{H_2L_c}$) shows maximum absorption bands in the range of 275-440 nm, were attributed to the π-π* transitions of the diazomethine chromophore and the benzene rings (intraligand charge transfer). Three intense bands were observed in the electronic spectra of each of the complexes at 255-430 nm for complex **1**, 260-420 nm for complex **2** and 370-440 nm for complex **3**. The spectra of complexes exhibit wide absorption bands with maximum at 340 and 255 nm for complex **1**, 335 and 260 nm for complex **2**, 320 and 270 nm for complex **3**, which are assigned to the intra-ligand π-π* and n-π* transitions, respectively. More-over, the charge transfer (CT) bands were also observed. The peaks assigned to metal-ligand charge transfers (MLCT) were observed at 430 nm for complex **1**), 420 nm for complex **2** and 440 nm for complex **3**.

Theortical biological studies: Computer models have been fostered as a valid alternative to experimental procedures for the predic-tion of ADME at the early steps of drug discovery [19]. A large variety of *in silico* methods share the objective of predicting ADME parameters from molecular structure and their pharma-cokinetic and physico-chemical parameters [20]. As potential application, the preliminary test for theoretical biological activities of synthesized disulfide ligands ($\mathbf{H_2L_a}$-$\mathbf{H_2L_c}$) and their corresponding metal (II) complexes have been evaluated by the computer model SwissADME [21] to compute physico-chemical descriptors as well as to predict ADME parameters, pharmacokinetic properties, drug-likeness and medicinal chemistry friendliness (among in-house proficient methods such as BOILED Egg, iLOGP and Bioavailability Radar) of one or multiple small molecules to support drug discovery.

The bioavailability radar outputs enables a first glance at the drug-likeness of molecules (Tables 2 and 3) based on well-absorbed and poorly absorbed, their lipophilicity and polarity as described by the *n*-octanol/water partition coefficient (log P) and the polar surface area (PSA). Coloured zone is the suitable physico-chemical space for oral bioavailability of the molecules. The pink area represents the optimal range for each properties [lipophilicity: XLOGP3 = 6.03, size: *m.w.* = 706.34 g/mol, polarity: TPSA = 215.10.48 Å^2, solubility: *log S* = -7.87 and flexibility: number of rotatable bonds = 9 for $\mathbf{H_2L_a}$; lipophilicity: XLOGP3 = 7.30, size: *m.w.* = 614.37 g/mol, polarity: TPSA = 115.78 Å^2, solubility: *log S* = -8.31, and flexibility: number of rotatable bonds = 7 for $\mathbf{H_2L_b}$; lipophilicity: XLOGP3 = 8.87, size: *m.w.* = 594.36 g/mol, polarity: TPSA = 126.59 Å^2, solubility: *log S* = -8.87 and flexibility: number of rotatable bonds = 7 for $\mathbf{H_2L_c}$; lipophilicity: XLOGP3 = 12.78, size: *m.w.* = 1176.78 g/mol, polarity: TPSA = 342.92 Å^2, solubility: *log S* = -14.70, and flexibility: number of rotatable bonds = 14 for (**1**); lipophilicity: XLOGP3 = 12.56, size: *m.w.* = 1000.80 g/mol, polarity: TPSA = 219.42 Å^2, solubility: *log S* = -13.78 and flexibility: number of rotatable bonds = 10 for (**2**); lipophilicity: XLOGP3 = 12.53, size: *m.w.* = 944.66 g/mol, polarity: TPSA = 236.28 Å^2, solubility: *log S* = -13.16 and flexibility: number of rotatable bonds = 12 for (**3**)]. These compounds are predicted not orally bioavailable, because too flexible and too polar structures.

The BOILED-Egg allows for intuitive evaluation of the passive gastrointestinal absorption (HIA) and brain penetration (BBB) in function of the molecules position in the WLOGP-*versus*-TPSA referential. The BOILED-Egg outputs for the synthesized disulfide derivatives ($\mathbf{H_2L_a}$-$\mathbf{H_2L_c}$) and its nickel(II) complexes (**1**-**3**) are given in Tables 2 and 3, respectively, which can be applied in a variety of settings at the early steps of drug discovery. On the basis of computed results presented in Tables 2 and 3, it is observed that the white region indicates the high probability of passive absorption by the gastrointestinal tract, and the yellow region (yolk) is for high probability of brain penetration in BOILED-Egg. Yolk and white areas are not mutually exclusive. In addition, the points are coloured in blue if predicted as actively effluxes by P-gp (PGP^+) and in red if predicted as non-substrate of P-gp (PGP^-). The synthesized disulfide ligands ($\mathbf{H_2L_a}$-$\mathbf{H_2L_c}$) were predicted as not absorbed and not BBB penetrant (outside the Egg) as compared with

TABLE-2
SwissADME COMPUTED PARAMETER IN THE DIFFERENT SECTIONS OF THE ONE-PANEL-PAR-MOLECULE OUTPUTS (PHYSICO-CHEMICAL PROPERTIES, LIPOPHILICITY, PHARMACOKINETICS, DRUG-LIKENESS AND MEDICINAL CHEMISTRY) FOR DISULFIDE LIGANDS

	H_2L_a	H_2L_b	H_2L_c
Physico-chemical properties			
Formula	$C_{26}H_{18}Br_2N_4O_6S_2$	$C_{26}H_{18}Br_2N_2O_2S_2$	$C_{26}H_{16}Cl_4N_2O_2S_2$
Molecular weight (g/mol)	706.34	614.37	594.36
Num. heavy atoms	40	34	36
Num. atom. heavy atoms	24	24	14
Fraction Csp^3	0.00	0.00	0.00
Num. rotatable bonds	9	7	7
Num. H-bond acceptors	8	4	4
Num. H-bond donors	4	2	2
Molar refractivity	165.92	151.44	156.08
TPSA (Å^2)	215.10	115.78	126.59
Lipophilicity			
log $P_{o/w}$ (iLOGP)	-10.22	3.44	3.97
log $P_{o/w}$ (XLOGP3)	6.03	7.30	8.43
log $P_{o/w}$ (WLOGP)	9.57	8.92	10.01
log $P_{o/w}$ (MLOGP)	3.75	5.56	6.29
log $P_{o/w}$ (SILICOS-IT)	3.71	7.98	9.20
Consensus log $P_{o/w}$	2.57	6.64	7.58
Water solubility			
log *S* (ESOL)	-7.87	-8.31	-8.87
Solubility (mg/mL; mol/L)	9.56×10^{-6}; 1.35×10^{-8}	3.02×10^{-6}; 4.92×10^{-9}	8.07×10^{-7}; 1.36×10^{-9}
Class (soluble)	Poor soluble	Poorly soluble	Poorly soluble
log *S* (Ali)	-10.33	-9.56	-10.73
Solubility (mg/mL; mol/L)	3.34×10^{-8}; 4.72×10^{-11}	1.70×10^{-7}; 2.77×10^{-10}	1.11×10^{-8}; 1.86×10^{-11}
Class (soluble)	Insoluble	Poorly soluble	Insoluble
log *S* (SILICOS-IT))	-9.22	-10.59	-11.38
Solubility (mg/mL; mol/L)	4.28×10^{-7}; 6.06×10^{-10}	1.59×10^{-8}; 2.58×10^{-11}	2.51×10^{-9}; 4.22×10^{-12}
Class	Poorly soluble	Insoluble	Insoluble
Pharmacokinetics			
GI absorption	Low	Low	Low
BBB permeant	No	No	No
P-gp substrate	Yes	Yes	Yes
CYP1A2 inhibitor	No	No	No
CYP2C19 inhibitor	No	Yes	No
CYP2C9 inhibitor	No	Yes	No
CYP2D6 inhibitor	No	Yes	Yes
CYP3A4 inhibitor	No	No	No
log K_p (cm/s) (skin permeation)	-6.33	-4.86	-3.94
Drug likeness			
Lipinski	Yes	No	No
Ghose	No	No	No
Veber	No	Yes	Yes
Egan	No	No	No
Muegge	No	No	No
Bioavailability score	0.56	0.17	0.25
Medicinal chemistry			
PAINS	0	0	0
Synthetic accessibility	4.03	3.66	3.83

standard drug (streptomycin with a TPSA of 331.43 Å^2 and a WLOGP of -7.74) while binuclear metal(II) complexes (**1**-**3**) was predicted as passively crossing the BBB (in yolk), but pumped-out from the brain (blue dot). One major role of P-gp is to protect the central nervous system (CNS) from xenobiotics. Importantly as well, P-gp is overexpressed in some tumour cells and leads to multidrug-resistant cancers. It has been suggested that cytochromes P450 (CYP) and P-gp can process small molecules synergistically to improve protection of tissues and organisms. The synthesized disulfide ligands (**H_2L_a**-**H_2L_c**) and its binuclear metal(II) complexes are substrate or inhibitor of isoenzymes governing important pharmacokinetic behaviours. Inhibitions of these isoenzymes are certainly one major cause of pharmacokinetics-related drug-drug interactions.

Biological studies: The synthesized disulfide ligands (**H_2L_a**-**H_2L_c**) and their corresponding binuclear metal(II) comp-

TABLE-3
SwissADME COMPUTED PARAMETER IN THE DIFFERENT SECTIONS OF THE ONE-PANEL-PAR-MOLECULE OUTPUTS (PHYSICOCHEMICAL PROPERTIES, LIPOPHILICITY, PHARMACOKINETICS, DRUG-LIKENESS AND MEDICINAL CHEMISTRY) FOR METAL COMPLEXES (**1**-**3**)

	Complex **1**	Complex **2**	Complex **3**
Physicochemical properties			
Formula	$C_{36}H_{27}Br_2Cl_2N_6Cu_2O_{14}S_2$	$C_{32}H_{24}Br_2Cl_2N_6Ni_2O_6S_2$	$C_{26}H_{19}Cl_6N_2Ni_2O_{12}S_2$
Molecular weight (g/mol)	1176.84	1000.80	944.66
Num. heavy atoms	64	52	50
Num. atom. heavy atoms	36	34	24
Fraction Csp^3	0.00	0.00	0.00
Num. rotatable bonds	14	10	12
Num. H-bond acceptors	18	10	14
Num. H-bond donors	3	2	3
Molar Refractivity	230.85	200.27	178.63
TPSA ($Å^2$)	342.92	219.42	236.28
Lipophilicity			
log $P_{o/w}$ (iLOGP)	0.00	0.00	0.00
log $P_{o/w}$ (XLOGP3)	12.78	12.56	12.53
log $P_{o/w}$ (WLOGP)	12.48	10.92	10.63
log $P_{o/w}$ (MLOGP)	-0.91	0.58	-0.64
log $P_{o/w}$ (SILICOS-IT)	1.96	6.22	7.44
Consensus log $P_{o/w}$	5.26	6.05	5.99
Water Solubility			
log *S* (ESOL)	-14.70	-13.78	-13.16
Solubility (mg/mL; mol/L)	2.36×10^{-12}; 2.00×10^{-15}	1.65×10^{-11}; 1.65×10^{-14}	6.54×10^{-11}; 6.91×10^{-14}
Class (soluble)	Insoluble	Insoluble	Insoluble
log *S* (Ali)	-20.01	-17.19	-17.52
Solubility (mg/mL; mol/L)	$1.14e \times 10^{-17}$; 9.68×10^{-21}	6.42×10^{-16}; 6.42×10^{-18}	2.89×10^{-15}; 3.05×10^{-18}
Class (soluble)	Insoluble	Insoluble	Insoluble
log *S* (SILICOS-IT))	-10.07	-11.45	-12.24
Solubility (mg/mL; mol/L)	1.01×10^{-7}; 8.59×10^{-11}	3.55×10^{-9}; 3.55×10^{-12}	5.43×10^{-10}; 5.74×10^{-13}
Class (soluble)	Insoluble	Insoluble	Insoluble
Pharmacokinetics			
Gl absorption	Low	Low	Low
BBB permeant	Yes	Yes	Yes
P-gp substrate	Yes	Yes	Yes
CYP1A2 inhibitor	Yes	Yes	Yes
CYP2C19 inhibitor	Yes	Yes	Yes
CYP2C9 inhibitor	Yes	Yes	Yes
CYP2D6 inhibitor	Yes	Yes	Yes
CYP3A4 inhibitor	Yes	Yes	Yes
log K_p (cm/s)	-4.42	-3.49	-3.17
Drug likeness			
Lipinski	No	No	No
Ghose	No	No	No
Veber	No	No	No
Egan	No	No	No
Muegge	No	No	No
Bioavailability score	0.17	0.17	0.17
Medicinal chemistry			
PAINS	0	0	0
Synthetic accessibility	5.43	4.66	4.55

lexes were investigated for their *in-vitro* antibacterial studies using agar disc diffusion method [12,13]. The antibacterial activities of compounds were determined against two bacterial strains (*E. coli* and *S. typhi*). These activities were determined at three concentrations *i.e.* 125 µg/mL (10 mM), 250 µg/ mL(15 mM), 375 µg/mL (20 mM) of each compounds in DMSO and results were compared with lower concentration of standard antibiotics (chloramphenicol drug) [22]. Each experiment was per-formed in triplicate. The radial growth of the colony was recorded on completion of the incubation and the mean diameter was recorded. DMSO (control) did not exhibited the clear inhibition zone. Each value was observed within the estimated error limits of ±1 mM. Comparable antibacterial screening results of the disulfide ligands (**H_2L_a-H_2L_c**) and its binuclear metal(II) comp-lexes are graphically presented in Fig. 5. The synthesized disulfide ligands (**H_2L_a-H_2L_c**) and its

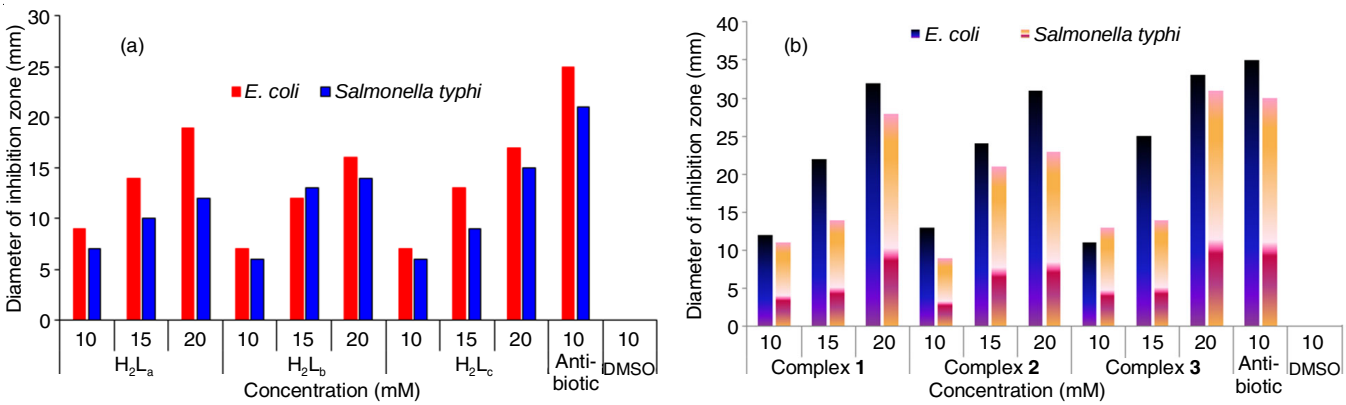

Fig. 5. Antibacterial activity of disulfide ligands (a) and its binuclear metal(II) complexes (**1-3**) (**H_2L_a-H_2L_c**) (b)

binuclear metal(II) complexes showed a lesser activity in 10 mM concentrations but showed an appreciable activity at higher concentrations. The disulfide ligands (**H_2L_a-H_2L_c**) inhibit the bacterial growth up to 13-20% μg mL^{-1} whereas other has poor antibacterial activity. It was observed that compound **H_2L_a** is more active than compound **H_2L_b** and **H_2L_c**. Similarly, binuclear metal(II) complexes (**1-3**) show a lower activity than the known antibiotics, with complex **3** being more active than complex **2** and complex **1**. This would suggest that chelation facilitate the activity of a compound to cross a cell membrane and can be explained by similar reports for antimicrobial activities [23,24]. On comparing the anti-bacterial activities of free disulfide ligands and its binuclear metal(II) complexes with these of standard bactericide, it was shown that binuclear metal(II) complexes had moderate activity as compared to standard drug but all the complexes were more active than disulfide ligands.

Antioxidant SOD activities: The antioxidant mimetic SOD activities of compounds were evaluated by NBT assay [25-29] using the reduction of NBT to MF^+ kinetically at 500 nm, as source of $O_2^{\bullet-}$ complexes showed IC_{50} values of 28, 32 and 36 mmol dm^{-3} for binuclear metal(II) complexes (**1-3**), respectively, which are higher than the value exhibited by the native Cu,Zn-SOD enzyme (IC_{50}= 0.04 mmol dm^{-3}). The catalytic activity of Ni-SOD, however, is near the same high level as that of Cu,Zn-SOD at about $10^9 M^{-1} S^{-1}$ per metal center [11]. Interestingly, disulfide derivatives (**H_2L_a-H_2L_c**) did not exhibit the SOD activity. Antioxidant SOD activities were also compared with the literature values [30-37]. Comparison of SOD values of these complexes is graphically presented in Fig. 6. The results indicated that the prepared complexes are more efficient antioxidant than vitamin C, which is the standard superoxide dismutase [37]. The antioxidant SOD activities of the present complexes may be attributed to the flexible nature of disulfide derivatives (**H_2L_a-H_2L_c**), which is able to accommodate the geometrical change from M(II) to M(I) in catalytic process. Complex **1** showed less IC_{50} value there by acts as a better catalysts of $O_2^{\bullet-}$ dismutation and hence yielded good SOD activity.

Mechanism: The catalytic function of binuclear metal(II) complexes can be understood according to the mechanism suggested in literature [37-39]. **Schemes II-IV** describes the

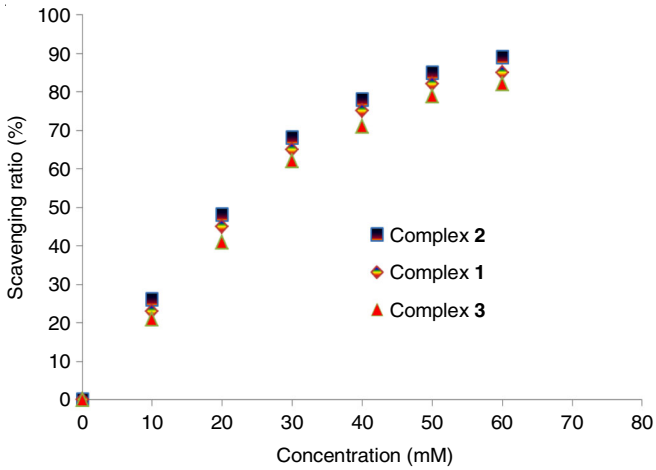

Fig. 6. SOD-like activity of binuclear metal(II) complexes (**1-3**) of disulfide ligands (**H_2L_a-H_2L_c**)

structural states for various steps of the $O_2^{\bullet-}$ disproportionation mechanism. The disproportionation of $O_2^{\bullet-}$ may take place in following steps: (i) $O_2^{\bullet-}$ displaces a pyridine/imidazole/water (for binuclear metal(II) complexes (**1-3**), respectively), binds directly to the M(II) ion and gives up its electron; (ii) the $O_2^{\bullet-}$ binding directly to the M(II) ion can be exchanged rapidly between the axial and the planar position of tetrahedral-like structure; (iii) the superoxide anion gives up its electron and forms neutral oxygen molecule leaves and M(II) reduced to M(I); (iv) a second $O_2^{\bullet-}$ binds again to the M(I) ion to accept an electron and a proton from the buffer. The second $O_2^{\bullet-}$ oxidizes M(I) to a M(II) species. These two species containing M(II) and M(I) centers remain in equilibrium. Since the proton exchange between the substrates and buffer is a rapid process, the $O_2^{\bullet-}$ further combines another proton from the solution to form a H_2O_2 molecule. Finally, the disulfide bridged tetrahedral Ni(II) reforms and electrically neutral H_2O_2 leaves from the system, completing a catalytic cycle.

Molecular docking simulation study: Molecular docking of the synthesized disulfide derivatives (**H_2L_a-H_2L_c**) were performed with active site of penicillin binding protein 4 (dacB; PDB id: 3A3I) and type II topoisomerase (gyrase B; PDB id: 5mmn) to predict their possible action of mechanism for the antibacterial property. The 3D atomic coordinates for the crystal

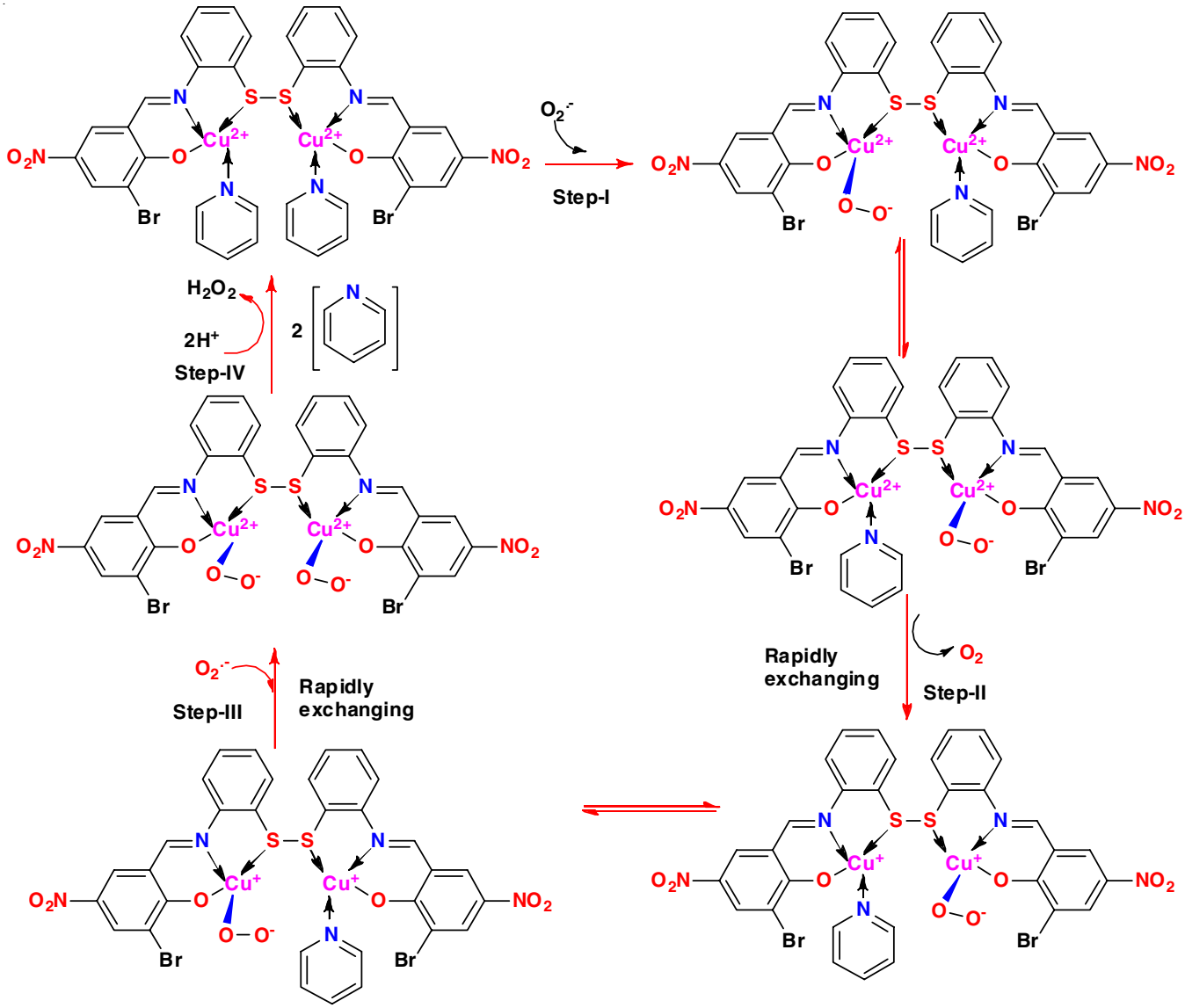

Scheme-II: A schematic mechanism of the suggested $O_2^{\bullet-}$ dismutation reaction catalyzed by complex **1** steering the $O_2^{\bullet-}$ to Cu(II)

TABLE-4
DOCKING RESULTS OF DISULFIDE COMPOUNDS AND THEIR CORRESPONDING COMPLEXES WITH PENICILLIN BINDING PROTEIN 4 (PBP4)

Compound name	BE (kcal/mol)	Ki	H-Bonding with PBP4 (critical residues in bold)
Ampicillin	-6.39	20.78 µM	**Ser423**, **Thr421,** Lys420**, Ser310**, **Ser69**, Lys425, Asp162
H_2L_a	-8.69	423.67 nM	**Ser423, Thr421, Ser69,** Lys420, **Ser310, Asn312,** Arg462
H_2L_b	-8.13	1.10 µM	**Ser310, Ser69, Ser423, Thr421,** Lys309**,** Arg462
H_2L_c	-8.94	281.44 nM	Asp162, Lys425, **Ser423,** Lys309, **Ser69**
H_2La Cu	-10.85	11.16 nM	**Ser69,** Lys420, Arg462, **Thr421**
H_2L_b Ni	-9.66	82.57 nM	Lys309**,** Arg462, **Thr421**
H_2L_c Ni	-9.44	119.80 nM	**Ser423,** Lys309, Asp162

structures of both targets were downloaded from RCSB-Protein Data Bank (PDB) [41,42]. The crystal structures of penicillin binding protein 4 (PBP4) and *E. coli* DNA Gyrase B 24 kDa ATPase domain were determined by X-ray diffraction method at 2 Å and 1.90 Å resolution, respectively. Molecular docking preparation and simulation were performed using UCSF Chimera and AutoDock 4.2 [43-47].

Docking with penicillin binding protein 4 (PBP4): The present molecular docking study was performed to evaluate the antibacterial property of synthesized disulfide derivatives (**H_2L_a-H_2L_c**) against penicillin binding protein 4 (PBP4) active site pocket. The docking scores of H_2La-H_2Lc were compared with ampicillin as reference molecule (Table-4). According to PDB structure deposited by Kawai *et al.* [41], ampicillin bound

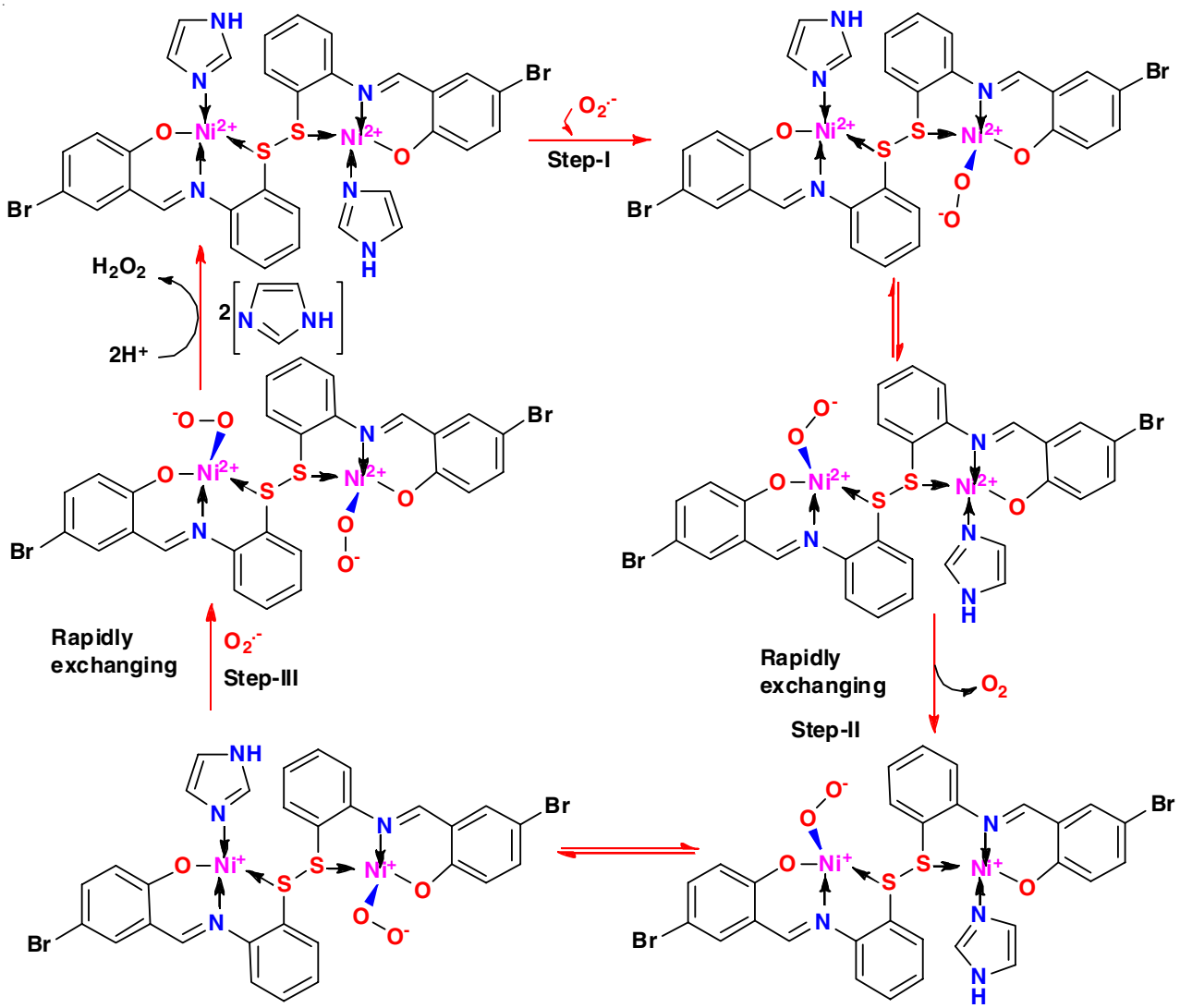

Scheme-III: A schematic mechanism of the suggested $O_2^{\bullet-}$ dismutation reaction catalyzed by complex **2** steering the $O_2^{\bullet-}$ to Ni(II)

TABLE-5
DOCKING RESULTS OF DISULFIDE COMPOUNDS AND THEIR CORRESPONDING COMPLEXES WITH DNA GYRASE B ATPase DOMAIN

Compound name	BE (kcal/mol)	Ki	H-Bonding (critical residues in bold)
Gyrase inhibitor	-8.00	1.38 µM	**Asp73**, Val71
H_2La	-7.48	3.27 µM	Arg136, **Val120,** Val97, Ser121, Asn46, Gly77, Thr165, **Arg76**, **Asp73,** Ile94**, Glu50**
H_2L_b	-9.27	160.22 nM	Asn46, **Val120, Asp73,** Asp49, **Glu50,** Arg136, **Arg76**
H_2L_c	-9.19	181.97 nM	**Asp73,** Asn46, **Val120,** Ile94**, Glu50,**
H_2La Cu	-9.46	116.20 nM	Arg136, Val97, Ser121, **Val120,** Gly77,
H_2L_b Ni	-7.56	2.89 µM	Asp49, Asn46, **Glu50, Arg76**
H_2L_c Ni	-7.97	1.43 µM	Asn46, **Glu50, Asp73**

to the active site pocket of PBP4 and established H-bonding with Ser423, Thr421, Ser310, Ser69, Asn312 residues which are critical for the inhibition of penicillin binding protein. All synthesized disulfide derivatives (**H_2L_a-H_2L_c**) were bound to the active site pocket of PBP4 as similar to the ampicillin molecule but with lower binding energy, hence displayed higher affinity toward the PBP4. They also exhibited similar H-bonding and hydrophobic interaction pattern as shown by ampicillin. Among the synthesized compounds, **H_2L_c** has shown the highest binding affinity for the PBP4 active site pocket.

Docking with type II topoisomerase (gyrase B): The molecular docking was also performed to explore the antibacterial property of synthesized disulfide derivatives (**H_2L_a-H_2L_c**) against *E. coli* DNA Gyrase B ATPase domain. The docking scores of **H_2L_a-H_2L_c** were compared with gyrase inhibitor as reference molecule. Molecular docking results of **H_2L_a-H_2L_c** and gyrase inhibitor with ATP-binding pocket of Gyrase B subunit are shown in Table-5. According to PDB structure deposited by Panchaud *et al.* [42], gyrase inhibitor (1-ethyl-3-[8-methyl-5-(2-methylpyridin-4-yl)isoquinolin-3-

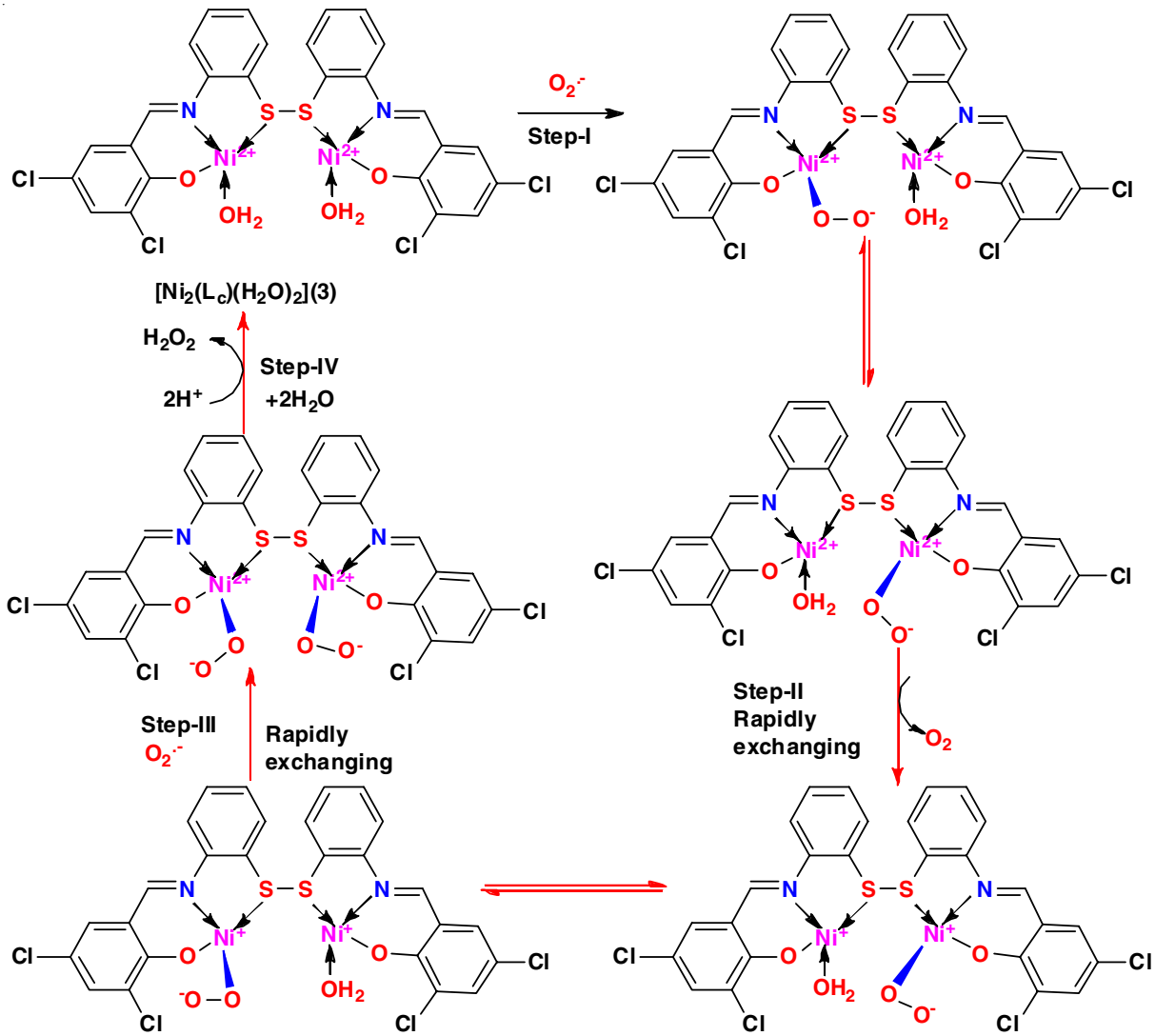

Scheme-IV: A schematic mechanism of the suggested $O_2^{\bullet-}$ dismutation reaction catalyzed by complex **3** steering the $O_2^{\bullet-}$ to Ni(II)

yl]urea) established H-bonds with Asp73, Glu50, Arg76 and Val120 residues present in the active site of the DNA gyrase B ATPase domain. Re-docking of gyrase inhibitor in the active site of gyrase B revealed that the molecule established two H-bonds with Asp73 residue and established hydrophobic contacts with Val71, Val167, Arg136, Glu50, Gly77, Arg76, Pro79, Thr165, Val43, Val120, Ile94, Asn46 and Ile78 residues in its lowest binding conformation. The residues Asp73 and Val120 are critical for the mediating inhibition. All synthesized disulfide derivatives ($\mathbf{H_2L_a}$-$\mathbf{H_2L_c}$) bound to the ATPase domain of gyrase B similar to the gyrase inhibitor. Two molecules $\mathbf{H_2L_b}$ and $\mathbf{H_2Lc}$ bound to the ATPase domain with lower binding energy compared to the gyrase inhibitor and $\mathbf{H_2L_a}$, hence displayed higher affinity toward the gyrase B. Among all the synthesized compounds, $\mathbf{H_2L_b}$ has shown the highest binding affinity for the ATPase domain. Molecular docking results of complexes are given in Tables 4 and 5. All the synthesized disulfide derivatives ($\mathbf{H_2L_a}$-$\mathbf{H_2L_c}$) exhibited similar H-bonding and hydrophobic interactions pattern as shown by the gyrase inhibitor.

Conclusion

In this study, we have designed and synthesized three new disulfide derivatives ($\mathbf{H_2L_a}$-$\mathbf{H_2L_c}$) and its binuclear metal (II) complexes (**1**-**3**). The use of auxiliary ligands (pyridine/imidazole/water molecule) in this metal-disulfide system led to the formation of binuclear metal(II) complexes with a disulfide-type ligands that links two metal centers. The SwissADME study of synthesized compounds $\mathbf{H_2L_a}$-$\mathbf{H_2L_c}$ and its binuclear metal(II) complexes were also carried out. Furthermore, new complexes (**1**-**3**) exhibit the catalytic activity toward the dismutation of superoxide anion and can be used as antioxidant SOD models for the pharmaceutical applications. Complex **1** shows higher antioxidant SOD activity as compared to complexes **2** and **3**.

ACKNOWLEDGEMENTS

The authors thank Department of Chemistry, NIT Patna, India for computational and spectral facilities.

CONFLICT OF INTEREST

The authors declare that there is no conflict of interests regarding the publication of this article.

REFERENCES

1. H. Seko, K. Tsuge, A. Igashira-Kamiyama, T. Kawamoto and T. Konno, *Chem. Commun.*, **46**, 1962 (2010); https://doi.org/10.1039/B913989C
2. C. Belle, W. Rammal and J.L. Pierre, *J. Inorg. Biochem.*, **99**, 1929 (2005); https://doi.org/10.1016/j.jinorgbio.2005.06.013
3. T. Kawamoto, M. Nishiwaki, M. Nishijima, K. Nozaki, A. Igashira-Kamiyama and T. Konno, *Chem. Eur. J.*, **14**, 9842 (2008); https://doi.org/10.1002/chem.200801614
4. T. Osako, Y. Ueno, Y. Tachi and S. Itoh, *Inorg. Chem.*, **42**, 8087 (2003); https://doi.org/10.1021/ic034958h
5. Y. Ueno, Y. Tachi and S. Itoh, *J. Am. Chem. Soc.*, **124**, 12428 (2002); https://doi.org/10.1021/ja027397m
6. A.M. Thomas, B.L. Lin, E.C. Wasinger and T.D.P. Stack, *J. Am. Chem. Soc.*, **135**, 18912 (2013); https://doi.org/10.1021/ja409603m
7. B.E. Kim, T. Nevitt and D.J. Thiele, *Nat. Chem. Biol.*, **4**, 176 (2008); https://doi.org/10.1038/nchembio.72
8. P. Faller and C. Hureau, *Dalton Trans.*, 1080 (2009); https://doi.org/10.1039/B813398K
9. A. Rauk, *Dalton Trans.*, 1273 (2008); https://doi.org/10.1039/b718601k
10. G. Meloni, P. Faller and M. Vašak, *J. Biol. Chem.*, **282**, 16068 (2007); https://doi.org/10.1074/jbc.M701357200
11. S. Bharti, M. Choudhary, B. Mohan, S.P. Rawat, S.R. Sharma and K. Ahmad, *J. Mol. Struct.*, **1164**, 137 (2018); https://doi.org/10.1016/j.molstruc.2018.03.041
12. B. Mohan, A. Jana, N. Das, S. Bharti and M. Choudhary, *J. Mol. Struct.*, **1171**, 94 (2018); https://doi.org/10.1016/j.molstruc.2018.06.016
13. S. Bharti, M. Choudhary and B. Mohan, *J. Coord. Chem.*, **71**, 284 (2018); https://doi.org/10.1080/00958972.2018.1424839
14. R.N. Patel, Y.P. Singh, Y. Singh, R.J. Butcher and M. Zeller, *RSC Adv.*, **6**, 107379 (2016); https://doi.org/10.1039/C6RA20367A
15. Y.P. Singh, R.N. Patel, Y. Singh, R.J. Butcher, P.K. Vishakarma and R.K.B. Singh, *Polyhedron*, **122**, 1 (2017); https://doi.org/10.1016/j.poly.2016.11.013
16. R.N. Patel, D.K. Patel, K.K. Shukla and Y. Singh, *J. Coord. Chem.*, **66**, 4131 (2013); https://doi.org/10.1080/00958972.2013.862790
17. A. Daina, O. Michielin and V. Zoete, *Sci. Rep.*, **7**, 42717 (2017); https://doi.org/10.1038/srep42717
18. F.F. Bentley, L.D. Smithson and A.L. Rozek, Infrared Spectra and Characteristic Frequencies ~700-300 cm^{-1}. A Collection of Spectra, Interpretation and Bibliography, Wiley & Sons: New York, Eds.: 1 (1968).
19. J.L. Dahlin, J. Inglese and M.A. Walters, *Nat. Rev. Drug Discov.*, **14**, 279 (2015); https://doi.org/10.1038/nrd4578
20. S. Tian, J. Wang, Y. Li, D. Li, L. Xu and T. Hou, *Adv. Drug Deliv. Rev.*, **86**, 2 (2015); https://doi.org/10.1016/j.addr.2015.01.009
21. A. Daina and V. Zoete, *ChemMedChem*, **11**, 1117 (2016); https://doi.org/10.1002/cmdc.201600182
22. K. Nomiya, R. Noguchi, K. Ohsawa, K. Tsuda and M. Oda, *J. Inorg. Biochem.*, **78**, 363 (2000); https://doi.org/10.1016/S0162-0134(00)00065-9
23. N.C. Kasuga, K. Sekino, C. Koumo, N. Shimada, M. Ishikawa and K. Nomiya, *J. Inorg. Biochem.*, **84**, 55 (2001); https://doi.org/10.1016/S0162-0134(00)00221-X
24. E. Bermejo, R. Carballo, A. Castiñeiras, R. Domínguez, C. Maichle-Mössmer, J. Strähle and D.X. West, *Polyhedron*, **18**, 3695 (1999); https://doi.org/10.1016/S0277-5387(99)00309-5
25. Y.-H. Zhou, X.-W. Liu, L.-Q. Chen, S.-Q. Wang and Y. Cheng, *Polyhedron*, **117**, 788 (2016); https://doi.org/10.1016/j.poly.2016.07.027
26. Y.-H. Zhou, J. Tao, D.L. Sun, L.-Q. Chen, W.G. Jia and Y. Cheng, *Polyhedron*, **85**, 849 (2015); https://doi.org/10.1016/j.poly.2014.10.010
27. M. Choudhary, R.N. Patel and S.P. Rawat, *J. Mol. Struct.*, **1070**, 94 (2014); https://doi.org/10.1016/j.molstruc.2014.04.018
28. M. Choudhary, R.N. Patel and S.P. Rawat, *J. Mol. Struct.*, **1060**, 197 (2014); https://doi.org/10.1016/j.molstruc.2013.12.043
29. R.G. Bhirud and T.S. Srivastava, *Inorg. Chim. Acta*, **179**, 125 (1991); https://doi.org/10.1016/S0020-1693(00)85383-9
30. R.N. Patel, Y.P. Singh, Y. Singh and R.J. Butcher, *Indian J. Chem.*, **54A**, 1459 (2015).
31. R.N. Patel, N. Singh, K.K. Shukla, V.L.N. Gundla and U.K. Chauhan, *Spectrochim. Acta A Mol. Biomol. Spectrosc.*, **63A**, 21 (2006); https://doi.org/10.1016/j.saa.2005.04.030
32. R.N. Patel, Y.P. Singh, Y. Singh, R.J. Butcher and J.P. Jasinski, *Polyhedron*, **129**, 164 (2017); https://doi.org/10.1016/j.poly.2017.03.054
33. R.N. Patel, Y.P. Singh, Y. Singh and B.J. Butcher, *Polyhedron*, **104**, 116 (2016); https://doi.org/10.1016/j.poly.2015.11.042
34. R.N. Patel, Y.P. Singh, Y. Singh, R.J. Butcher, M. Zeller, R.K.B. Singh and O. U-wang, *J. Mol. Struct.*, **1136**, 157 (2017); https://doi.org/10.1016/j.molstruc.2017.01.083
35. Y.P. Singh, R.N. Patel, Y. Singh, D. Choquesillo-Lazarte and R.J. Butcher, *Dalton Trans.*, **46**, 2803 (2017); https://doi.org/10.1039/C6DT04661D
36. I.A. Koval, P. Gamez, C. Belle, K. Selmeczi and K. Reedijk, *Chem. Soc. Rev.*, **35**, 814 (2006); https://doi.org/10.1039/b516250p
37. Y. Li, Z.Y. Yang and J.C. Wu, *Eur. J. Med. Chem.*, **45**, 5692 (2010); https://doi.org/10.1016/j.ejmech.2010.09.025
38. P.J. Hart, M.M. Balbirnie, N.L. Ogihara, A.M. Nersissian, M.S. Weiss, J.S. Valentine and D. Eisenberg, *Biochemistry*, **38**, 2167 (1999); https://doi.org/10.1021/bi982284u
39. L.M. Ellerby, D.E. Cabelli, J.A. Graden and J.S. Valentine, *J. Am. Chem. Soc.*, **118**, 6556 (1996); https://doi.org/10.1021/ja953845x
40. U.L. Weser, M. Schubotz and E. Lengfelder, *Eur. J. Mol. Catal.*, **13**, 249 (1981); https://doi.org/10.1016/0304-5102(81)85025-0
41. F. Kawai, T.B. Clarke, D.I. Roper, G.J. Han, K.Y. Hwang, S. Unzai, E. Obayashi, S.Y. Park and J.R. Tame, *J. Mol. Biol.*, **396**, 634 (2010); https://doi.org/10.1016/j.jmb.2009.11.055
42. P. Panchaud, T. Bruyère, A.C. Blumstein, D. Bur, A. Chambovey, E.A. Ertel, M. Gude, C. Hubschwerlen, L. Jacob, T. Kimmerlin, T. Pfeifer, L. Prade, P. Seiler, D. Ritz and G. Rueedi, *J. Med. Chem.*, **60**, 3755 (2017); https://doi.org/10.1021/acs.jmedchem.6b01834
43. B. Mohan, M. Choudhary, G. Kumar, S. Muhammad, N. Das, K. Singh, A.G. Al-Sehemi and S. Kumar, *Synth. Commun.*, **50**, 2199 (2020); https://doi.org/10.1080/00397911.2020.1771369
44. I. Gaurav, T. Singh, A. Thakur, G. Kumar, P. Rathee, P. Kumari and K. Sweta, *Curr. Pharm. Biotechnol.*, **21**, 1674 (2020); https://doi.org/10.2174/1389201021666200702152000
45. G. Kumar, P. Paliwal, N. Patnaik and R. Patnaik, *J. Theor. Comput. Chem.*, **16**, 1750042 (2017); https://doi.org/10.1142/S0219633617500420
46. S. Kumar, G. Kumar and I.C. Shukla, *SN Appl. Sci.*, **2**, 1241 (2020); https://doi.org/10.1007/s42452-020-3067-7
47. S. Kumar, G. Kumar, A.K. Tripathi, S. Seena and J. Koh, *J. Mol. Struct.*, **1157**, 292 (2018); https://doi.org/10.1016/j.molstruc.2017.12.067